Identifying the Cruising Dynamics of a Medium Scale UAV I: Longitudinal Dynamics

C. I. Gamage, S. C. Samarasekera, A. Tennakoon, R. Lalantha, and R. Munasinghe
Unmanned Aerial Vehicles Research Laboratory
Department of Electronics and Telecommunication
University of Moratuwa
Katubadda, Sri Lanka

***Abstract*— Pitch and airspeed responses of a medium scale UAV were identified using the prediction error method. Data collection was conducted with an active closed loop autopilot control system. A naive SISO open loop transfer function was estimated using the parametric direct approach. Since its predictability was not significant, better estimators were developed using MISO parametric direct, and SISO parametric indirect method. The model validations were done to quantify their predictability.**

***Keywords*— MUAV, System identification, closed loop identification, indirect method**

I. INTRODUCTION

System Identification plays a vital role in airframe design and development. While the initial airframe design is guided by theoretical calculations and computational fluid dynamics simulations, its verification and fine tuning is done via system identification. These experiments estimate system constants using repeated flight tests under different conditions. The vehicle dynamics are excited using the throttle and the control signals to the aileron, elevator, and the rudder. An onboard data logger will measure the aircraft state, which typically includes its translational and rotational velocities, aerodynamic angles, and its attitude. These control inputs and their respective responses from multiple experiments are used to estimate the system coefficients.

There is a wide variety of aircraft types, each with different system dynamics. The two main classes; fixed wing and rotorcrafts have very different systems models. Even within the same aircraft type, different scales, payload capacity, and response time gives rise to distinct system dynamics. All these characteristics should fit the mission at hand, and system identification process enables the developer to give the necessary quality assurance of the aircraft. In this work we will focus on a medium scale unmanned aircraft, ddeveloped by the UAV Lab of University of Moratuwa. Named as Robotic Ariel Vehicle for Autonomous Navigation (RAVAN), its primary mission is to facilitate as a research platform for the development of efficient navigation algorithms.

978-1-4799-1740-2/15/$31.00 ©2015 IEEE

Fig. 1. Robotic Ariel Vehicle for Autonomous Navigation *(RAVAN)*

The aircraft consist of a twin-boom airframe with a vertical stabilizer. The airframe components have simple geometry which makes it relatively easy to fabricate. Its moderate aspect ratio (the ratio of the wing's length to its breath) gives a good balance between gliding and maneuvering.

RAVAN is powered by an 8000mAh 24V LiPo battery and propelled by a 1.5kW brushless DC motor. This power system is constrain the maximum flight time for about 20 minutes. The aircraft is equipped with the open source Ardupilot autopilot system, which uses an ArduIMU for inertial measurements. The inertial measurement unit (IMU) houses a 3 axis gyro and a 3 axis accelerometer. These two measurements are fused using a direction cosine filter [3] to estimate the aircraft attitude. An onboard GPS estimates the aircraft's current position, a pitot tube is used to estimate the (longitudinal) airspeed, and a barometer estimates the altitude.

The aircraft has now logged more than 20 hours of flight time in altitudes up to about 200m facilitating different navigation algorithms. The take-off and landing is controlled manually via remote control. After climbing up to the designated altitude the autopilot system is activated and the aircraft will navigate over a set of preprogrammed waypoints. The team is now focusing on optimizing the airframe and controllers for commercial deployment. It is well established that system

identification of small and medium scale UAV's can facilitate better controllers [6, 7, 8, and 9].

The full Degree of freedom (DOF) airframe system identification problem is formulated using the rigid body equations of motion for the aircraft, which gives a set of nonlinear equations. These are then linearized via a perturbation analysis about a trim flight condition. The usual trim condition is the level flight with longitudinal stability [1, 2]. This gives rise to the aerodynamic coefficients that linearly relate the aerodynamic forces and torques to the dynamic variables of the airframe; airspeed, aerodynamic angles, control surface rotations, and the angular rates [1]. An overview of these coefficients are given in Table 1. For fixed wing aircrafts like RAVAN the problem can be decoupled in to two 3 DOF problems, namely longitudinal motion and the lateral motion [1].

From Table I it can be observed that for a full specification of system dynamics one needs to observe the two aerodynamic angles, the angle of attack and the slide-slip angle. Angle of attack is the angle between aircraft heading and the airspeed vector, and the slide slip angle is the angle between the airspeed vector and the body axis on horizontal plane. Estimating both these angles require the measurement of all three components of the airspeed vector. But currently RAVAN is equipped with only one airspeed sensor which gives its head-on airspeed component. This severely limits our capability to identify the total system dynamics using the classical method, due to unavailability of the input variables. Real-time system identification with such a constrain is almost impossible in practice as even with zero wind speeds at the ground level the wind speeds at the flying altitude can vary a lot.

This motivate us to look at the "black box" system identification which tries to model the system using available inputs and outputs [4]. While a suitably simple model can be identified for any given set of inputs and outputs, the model developer should look for any spurious relationships that do not arise from the underlying physics [4]. Several tools are available to detect and avoid this pitfall. For proper identification of an airframe, the domain literature refers to correct specification of the following components of the identification procedure [1, 2],

- Model: The system model should be physically plausible for the type of vehicle
- Maneuver: Input signals must have proper bandwidth that cover all dominant modes of the system responses modeled (persistent excitation of the system),
- Measurements: Adequate instrumentation for measurement and recording of the dynamic variables with sufficient accuracy.
- Method: A suitable identification (error) criterion, and a computational algorithm that converge on its minimum.

TABLE I. AERODYNAMIC COEFFICIENTS AND UNDERLYING DYNAMIC VARIABLES THAT GOVERN THEM

Coefficient	Governing Dynamic variables
Thrust force	Airspeed
Lift force	angle of attack
Lateral force	slide slip angle
Drag force	angle of attack, slide slip angle
Roll torque	Aileron deflection, slide slip angle, roll axis turn rate, yaw axis turn rate
Pitch torque	Elevator deflection, angle of attack, pitch axis turn rate
Yaw torque	Rudder deflection, Yaw turn rate, slide slip angle

For a detail discussion of these aspects of experiment design and parameter estimation the reader is referred to [1, 2].

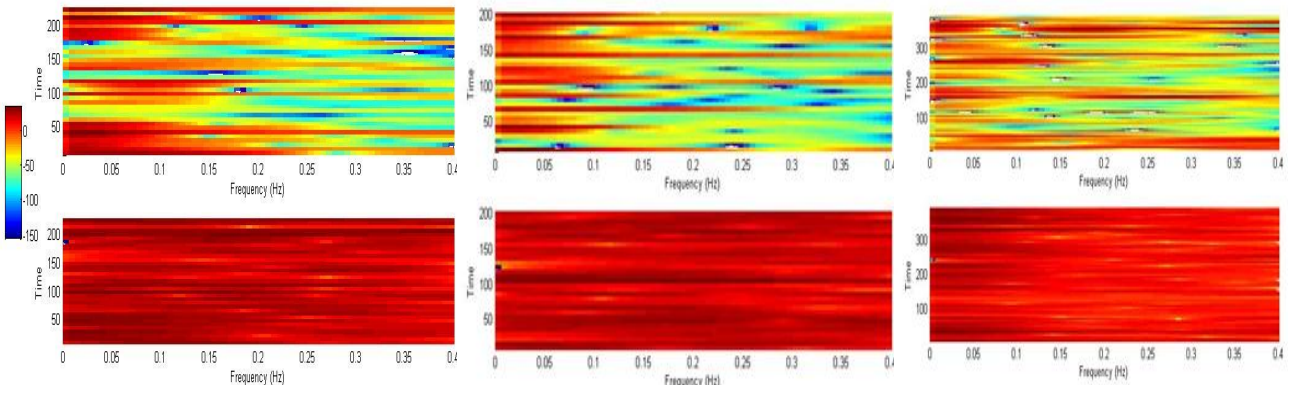

Fig. 2. Spectrogram of experiment 1,4,5 *(calculated with window = Hamming, window length = 8)*. The top row shows the time frequency variations of roll while the bottom row shows the time frequency variations of the pitch.

II. DATA COLLECTION AND CORRELATION ANALYSS

UAV lab has a good database of flight records generated from the waypoint navigation experiments. Therefore the initial system identification efforts are aimed at using this existing data set. Since any proper model estimate would have to be asymptotically consistent (approaching the true model as the number of data points increase) [1, 2, 4] such an approach seemed to be a good starting point.

The data set contains time stamped values of the measurements from the IMU (roll, pitch yaw) , GPS (latitude, longitude, ground speed), barometer (altitude), pitot tube (air speed) and the system commands from the auto pilot namely; the reference airspeed, reference altitude, flying mode (manual or automatic), Thrust percentage, and the control surface (aileron and elevator) deflections. Note the absence of rudder deflections in the data set. This is because the rudder was coupled with the aileron for efficient banking turn control in waypoint navigation.

In the current data set, the input output signal spectra generated by the autopilot at the cruising altitude, and by the manual pilot during the takeoff and landing stage. This switch of control together with the different modes that dominate at different flight stages actually demands a more tailored control command sequences [1, 2]. We only included the cruising flight data in our analysis, which is the data segment that corresponds to the autonomous flight. We also experimented with data from totally manual experiments, which confirmed our need for further development of excitation waveforms.

Since we cannot observe the angle of attack and slide slip angle we opted to filter out data sets with high wind conditions. Note that we did this *a posteriori* to the experiment. Due to the considerable flight time the pilot and the flying team were able to detect zero wind conditions by the banking turn characteristics of the aircraft. Further, the experiments were conducted at the same venue which enabled us to identify certain patterns in the wind conditions. For example the flying altitude wind on a normal clear sky day would only pick up after a certain time.

TABLE II. THE AVERAGE (μ) AND THE STANDARD DEVIATION (Σ) OF THE SIGNIFICANT CROSS CORRELATIONS ACROSS DIFFERENT EXPERIMENTS

Parameter pair	**μ**	**σ**
Airspeed – Throttle	0.6777	0.0742
Airspeed – Pitch	0.6347	0.0883
Altitude – Pitch	-0.3567	0.2948
Altitude - Throttle	-0.4324	0.3453
Pitch – Throttle	0.7369	0.0755
Pitch - Elevator	-0.5805	0.1587
Roll – Aileron	-0.3176	0.1587
Roll - Longitude	0.2499	0.1581
Altitude - Longitude	0.2002	0.3543
Latitude - Longitude	-0.4236	0.1175

Using this *a posteriori* analysis of banking angle and time of flight we were able to find 10 flight experiments that had almost zero wind at the flying altitude. We took 5 data sets for model estimation and kept the other 5 for model validation.

In order to formulate a realistic observable model we analyzed the cross correlations between the input and output variables. This enabled us to pair up variables for system modeling and identify any spurious patterns that would limit system identification. The mean (μ) and the standard deviation (σ) of significant cross correlations between the dynamic variables across the experiments are given in Table 2.

It can be observed that the σ(Airspeed, Throttle), σ(Airspeed, Pitch), and σ(Pitch, Throttle) are considerably low. This suggests that the corresponding high correlations are robust for unobserved disturbances across experiments. Note the significant cross correlations among the latitude, longitude and altitude. These are data artifacts arising from navigation path patterns. The more concerning factor is the significant correlation between roll and longitude that occurs as a result of banking at the waypoints, of the repetitive navigation patterns. This questions the persistent excitation of aileron deflection within the data set. As a diagnostic we compared the spectrograms of the aileron deflection to the spectrograms of the elevator deflection, in 3 typical experiments. The spectrograms are given in Figure 2, which clearly shows that the spectral content of the aileron deflection is in fact quite limited compared to the elevator deflection. This led to our concentration on identifying the longitudinal dynamics only.

III. ESTIMATION OF PITCH AND AIRSPEED RESPONSES

As we concentrate solely on the longitudinal dynamics of the RAVAN airframe, a sensible starting point would be to estimate airspeed transfer function G_{uA}, and the elevator servo deflection to pitch angle transfer function $G_{u\theta}$, where the subscript u denote the respective inputs. From Table I and II we can formulate that throttle command govern the airspeed, and elevator command govern the pitch. Thus we can formulate our problem as finding $G_{T\Delta a}$ and $G_{E\theta}$. One might argue that the airspeed do correlate with pitch, but the average (zero lag) cross correlation between airspeed and elevator signal is only 0.0307.

We adopted time domain parametric model structures as our model space. The other option would have been to take the spectral approach, which would require us to do a set of experiments using chirp signals to estimate the system transfer functions [1]. While this method is popular among advanced aircraft designs, it require special experiment environments (e.g. wind tunnels, constrained flights) for initial estimates of the airframe bandwidth without damaging the airframe. But the trade-off is computational complexity of the estimating algorithm.

Due to the predictor simplicity and guaranteed convergence we chose to impose an ARMAX structure (Autoregressive moving average with input filtering) [4] for the transfer

functions. For an input **u**[n], output **y**[n] and noise **e**[n] these models take the form

$$\mathbf{A}(z^{-1})\,\mathbf{y}[n] = \mathbf{B}(z^{-1})\,\mathbf{u}[n] + \mathbf{H}(z^{-1})\,\mathbf{e}[n] \quad (1)$$

where z^{-1} is the shift (delay) operator, and n refers to the discrete time sequence index. The matrices **A**, **B** and **H** are finite impulse response (FIR) filters that approximate system response. The transfer function can be found as

$$\mathbf{G}(z^{-1}) = \mathbf{A}^{-1}(z^{-1})\,\mathbf{B}(z^{-1})$$

and it's common to assume that the noise spectrum is white, with the noise filter $\mathbf{H}(z^{-1})$ modeling the output trends that are not accounted by linear transformations of the model inputs. The use of delay operator and time indexing in the same equation might seem as an abuse of notation, but due to its practicality, this representation is the norm in the system identification and fault diagnostics communities. In (1) and the rest of the paper bold capital letters denote transfer functions, which can be matrices, vectors or scalars accordingly, bold simple letter denote vectors and normal font denote scalars.

To find the best fit, we adopted the prediction error minimization (PEM) technique [2, 4] which is quite customary for airframe system identification [2, 4, 6, 7, 8, 9]. The polynomial order n (the number of delay elements in each FIR polynomial) was found by finding the Akaike information coefficient over a grid. This is a minimum square error measure compensated with a cost per additional parameter. The axis's were limited to max (n_A) = 10, max (n_B) = 10, max (n_H) = 5 due to computational considerations.

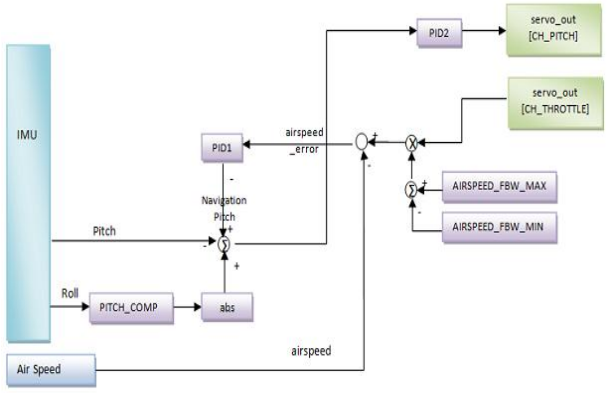

Fig. 3. Air speed control loop. Sample time = 1.25s. The PID is with integal winding up.

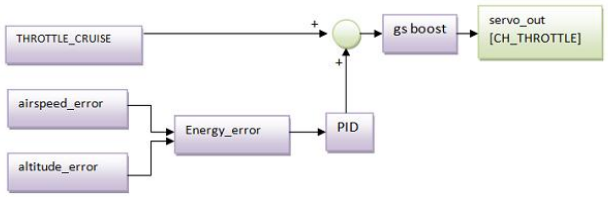

Fig. 4. Pitch control loop. The PID is with integal winding up.

Although the airframe itself is a continuous time system we have opted to model the system in discrete time due to the sampled nature of the time series. This is because of the fact that the identified system would be used in computer simulations for predicting aircraft maneuverability [5], and driving a digital control system for better path navigation [6] For this a sufficiently high sample rate discrete time representation of the system model would suffice

While the PEM estimates do converge with low estimator covariance, it is shown in the model validation section that this single input single output (SISO) models are unable to capture much of the pitch and airspeed dynamics. This severely limits their utility in simulators, predictors and a controllers. This leads to the development of a model considering all respective significantly correlated (cross correlation > 0.2) variables for pitch and airspeed as inputs. This might seems unnatural as it is only the thrust and the elevator deflection that actually act as control inputs.

We further improved the resulting model's predictability by replacing the airspeed and altitude with their error signals relative to levels. This can be a result of airspeed error and altitude error being the actual output signal of interest in the cruising mood which the auto pilot is actually trying to minimize. Since the cruising altitude and speed was programed *a priori* it was a simple level shift.

The PEM estimates of the model polynomials for pitch were found to be

$\mathbf{y_p} = p$

$\mathbf{u_p} = [\text{Elevator deflection, Airspeed error, Roll, Altitude error}]^T$

$\mathbf{A_p} = 1 - 0.6911z^{-1} - 0.8143z^{-2} + 0.4461z^{-3} + 0.06149z^{-4}$

$\mathbf{B} = [\mathbf{B}_{ep}, \mathbf{B}_{\Delta ap}, \mathbf{B}_{rp}, \mathbf{B}_{\Delta zp}]^T$

$\mathbf{B}_{ep} = -0.5276 + 0.372z^{-1} + 0.4537z^{-2} - 0.22391^{z-3} - 0.05659z^{-4}$

$\mathbf{B}_{\Delta ap} = -0.693 + 0.2646z^{-1} + 0.6814z^{-2} - 0.1236z^{-3} - 0.1285z^{-4}$

$\mathbf{B}_{rp} = -0.01656 + 0.008333z^{-1} + 0.008112z^{-2}$

$\mathbf{B}_{\Delta zp} = -0.01983 - 0.03793z^{-1} + .04753z^{-2} + 0.02482z^{-3} - 0.0148z^{-4}$

$\mathbf{H}_p = 1 - 0.1643z^{-1} - 0.8151z^{-2}$

where $\mathbf{B}_{ep}$ is the elevator deflection to pitch transfer function, $\mathbf{B}_{\Delta ap}$ is the airspeed error to pitch transfer function, $\mathbf{B}_{rp}$ is the roll to pitch transfer function, and $\mathbf{B}_{\Delta zp}$ is the altitude error to pitch transfer function.

The PEM estimates of the model polynomials for Δa were found to be,

$\mathbf{y}_{\Delta a} = \Delta a$

$\mathbf{x}_{\Delta a} = [\text{throttle, pitch, ground speed}]^T$

$\mathbf{A}_{\Delta a} = 1 - 1.265z^{-1} + 0.1877z^{-2} + 0.1156z^{-3} + 0.07345z^{-4} + 0.1114z^{-5}$

$\mathbf{B} = [\mathbf{B}_{t\Delta a}, \mathbf{B}_{p\Delta a}, \mathbf{B}_{g\Delta a}]^T$

$\mathbf{B}_{t\Delta a} = -0.04028 + 0.009745z^{-1} + 0.0298z^{-2} - 0.01759z^{-3} - 0.01688z^{-4}$

$\mathbf{B}_{p\Delta a} = -0.09143 + 0.09094z^{-1}$

$\mathbf{B}_{g\Delta a} = -0.001074 + 0.001056z^{-1}$

$\mathbf{H}_{\Delta a} = 1 - 0.7499z^{-1} - 0.2381z^{-2}$

where $\mathbf{B}_{t\Delta a}$ is the throttle to airspeed error transfer function, $\mathbf{B}_{p\Delta a}$ pitch to airspeed error transfer function, and $\mathbf{B}_{g\Delta a}$ ground speed to airspeed error transfer function. The presence of other system output variables in the inputs is due to the close loop control via the auto pilot. The two control loops are given in Fig. 3 and Fig. 4.

System identification via closed loop control do present few additional challenges. The main reason is the high correlations between components of **y** and **u**. This can be explained via the following closed loop control equations of the system.

$$\mathbf{y}[n] = \mathbf{G}(z^{-1})\,\mathbf{u}[n] + \mathbf{H}(z^{-1})\mathbf{e}[n] \qquad (2.a)$$

$$\mathbf{u}[n] = \mathbf{r}[n] - \mathbf{C}(z^{-1})\mathbf{y}[n] \qquad (2.b)$$

where $\mathbf{r}[n]$ is the reference signal to the controller and $\mathbf{C}(z^{-1})$ is the feedback controller. Adopting the open loop system identification approach to a closed loop controlled systems is known as the direct method. Direct method would be consistent only if $\mathbf{r}[n]$ sufficiently excite the controller, $\mathbf{C}(z^{-1})$ is of sufficiently high order and $\mathbf{C}(z^{-1})$ switches between several modes within the experiment [10,11]. In other words the spectrums of the reference and the controller output signals should be significant within the system bandwidth. In order to reduce the resulting asymptotic bias the signal to noise ratio of the controller output should be large, and the noise filter model $\mathbf{H}(z^{-1})$ should be independent from the system response parameters [6, 11, 12]. While the first condition is readily achieved in microcontroller based digital control systems, achieving the second condition pose some challenges as all significant parameter dependent inputs should be considered for successful system identification. This caused the poor performance of the single input models, and the significant increase in performance as more inputs were used.

The knowledge of the closed loop control system allows us to further break the variables that influence the system excitation in to direct inputs $\mathbf{u}[n]$ and variables that influence the controller reference input $\mathbf{r}[n]$. This simpler model by isolating the r[n]. This is known as the indirect method within the domain literature [5, 6, 9, and 10]. To do this, we first rearrange the terms in (2.a) (2.b) using the inverse sensitive function $\mathbf{S}(z^{-1}) = 1 + \mathbf{G}(z^{-1}).\mathbf{C}(z^{-1})$

$$\mathbf{S}(z^{-1})\mathbf{y}[n] = \mathbf{G}(z^{-1})\mathbf{r}[n] + \mathbf{H}(z^{-1})\mathbf{e}[n] \qquad (3a)$$

$$\mathbf{S}(z^{-1})\mathbf{u}[n] = \mathbf{r}[n] - \mathbf{C}(z^{-1})\mathbf{H}(z^{-1})\mathbf{e}[n] \qquad (3b)$$

We used a two stage estimation method similar to [9], where we first identified the polynomials S and G using (3a). We could have gone to identify $\mathbf{C}(z^{-1})$ using (3b). Since we already know the controller structure we stop just using the first stage of this two stage method. Note that (3a) is already in the ARMAX form. Therefore we recreated $\mathbf{r}[n]$ by implementing the control loops in Fig. 3 and Fig. 4, which are slight modifications of the open source Ardupilot[tm] controller code. We then performed a PEM ARMAX identification based on $\mathbf{y}[n]$ and $\mathbf{r}[n]$. The model orders were again determined using a grid search to find the minimum Akaike information coefficient parameterization. It should be noted that a relatively high order inverse sensitivity function polynomial with $n_S = 28$ was needed in order to get consistent estimators. This can be attributed to the integral terms in the PID loops. The resulting transfer functions were

$\mathbf{G}_{ep}(z^{-1}) = -0.5635 - 0.04976z^{-1} + 0.3546z^{-2} + 0.2995z^{-3} - 0.04627z^{-4} - 0.03923z^{-5}$

$\mathbf{G}_{t\Delta a}(z^{-1}) = -0.496 - 0.35z^{-1} + 0.2502z^{-2} - 0.03435z^{-3} - 0.9972z^{-4} - 0.09689z^{-5}$

IV. MODAL VALIDATION

We have developed 3 models for the pitch response and the airspeed error response of RAVAN. While PEM ARMAX estimates do converge to a local minima with ease, the real challenge is to verify their consistency. One practical measure of their utility is to look at how well the model predict the output for data sets not used in the estimation. As a good approximation would already be in the local neighborhood of the true model parameters it would be valid in these new cases too. Note that we used only 5 out of the 10 experiments for the parameter estimation. We now use the other 5 experiments as validation data sets. These experiments were done on different days under different conditions, with the only common parameter value being the low atmospheric wind.

The model validation plots for the MISO open loop model is given in Figure 5. For brevity of presentation we don't present other plots, but as a summery measure of fit we use the R^2 statistic. An R^2 value close to one would mean a good fit [4]. The R^2 statistics for the 5 experiments using the 3 models are given in Table 3. One can see that the R^2 values of multi input open loop method is much better than the single excitation method. Using the control loop information does enable us to reduce the model complexity and achieve comparable fits to the multi input open loop model. But it should be noted that

in some experiments the open loop multi input systems show better fit than the closed loop system.

V. CONCLUSION AND FUTURE WORK

The longitudinal system responses of RAVAN was estimated. We evaluated 3 candidates starting from a naïve open loop estimator, multi input responses and then looked at response estimation with control loop information. It should be noted that while using the control loop information did allow us to arrive at a simpler model. it's validity should be verified with more experiments with wider variety of excitations. Finding the lateral dynamics pose some new challenges as we need to design the Quad- M s to catch the dominant modes of the airframe. We also are in the process of retrofitting RAVAN with multiple airspeed sensors that would enable full measurement of the wind vector which enable us to identify the physically based "Gray box" model and provide the classic full order of aerodynamic constants for RAVAN. In this first stage our focus is only on cruising dynamics only as the autopilot is activated at only this mode. With the development of autonomous landing and take of controller, we would be able to provide precise system excitations in these flight moods enabling us identify the general systems model.

TABLE III. R^2 VALUES OF DIFFERENT MODELS FOR THE VALIDATION DATA SET. (FIRST ROW GIVES THE PITCH VALIDATION VALUES AND THE SECOND ROW GIVES THE AIRSPEED VALIDATION VALUES)

Model	exp. 6	exp.7	exp. 8	exp. 9	exp. 10
Direct method SISO	0.1120	0.2700	0.1029	0.0016	0.2301
	0.0341	0.056	0.4588	0.0671	0.0340
Direct method MISO	0.4958	0.5858	0.5042	0.5393	0.5928
	0.4771	0.4201	0.3816	0.3551	0.3619
Indirect method SISO	0.6580	0.5521	0.3616	0.4530	0.2210
	0.6030	0.5899	0.5621	0.3031	0.2101

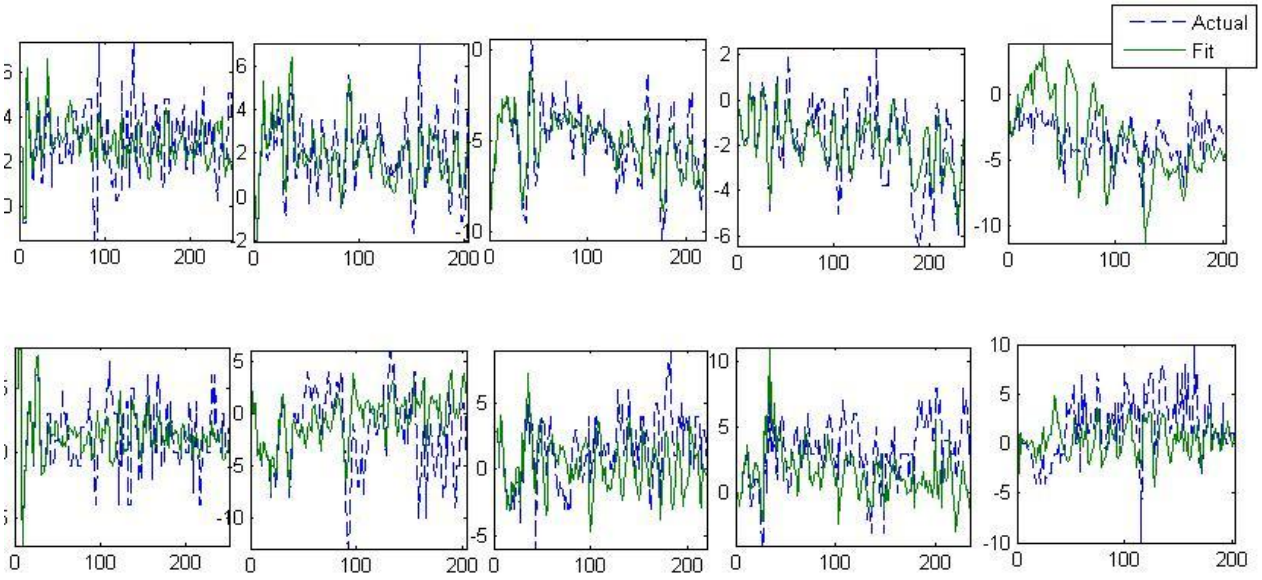

Fig. 5. Air speed error and ptich MISO model validation plots. The 1st row gives the airspeed data/fits, and 2nd row shows the pitch data/fits. The x axis is time in ms. the Air speeds are in kmph and pitch is in degrees.

ACKNOWLEDGMENT

The authors would like to thank Laxman Swarnakumara, for his service as the RC pilot during the experiments and Sanjeewa Fernando for his technical assistance in conducting flight experiments. This research was funded by the Senate Research Committee of the University of Moratuwa under grant SRC/LT/2014/09

REFERENCES

[1] M. B. Tischler, and R. K. Remple, *Aircraft and Rotorcraft System Identification : Engineering Methods with Flight-Test Examples*. Reston, VA: AIAA. 2006.

[2] R.V. Jategaonkar, *Flight Vehicle System Identification - A Time Domain Methodology - Progress in Astronautics and Aeronautics*, Volume 216. VA:AIAA. 2006

[3] R Mahony, T. Hamel, J Pflimlin, "Complementary filter design on the special orthogonal group SO(3)," Decision and Control, 2005 and 2005 European Control Conf.. CDC-ECC '05, Seville, 2005 pp.1477-1484

[4] Lennart Ljung, *System Identification: Theory for the User* ,2nd ed, NJ: Prentice Hall, 1999.

[5] Urban Forssell, Lennart Ljung, "Closed-loop identification revisited", Automatica, Volume 35, Issue 7, Pages 1215-1241, July 1999,

[6] Grymin, D.J.; Farhood, M., "Two-step system identification for control of small UAVs along pre-specified trajectories," Amer. Control Conf. , pp.4404 - 4409, 2014

[7] Andrei Dorobantu, Austin Murch, Bérénice Mettler, and Gary Balas "System Identification for Small, Low-Cost, Fixed-Wing Unmanned Aircraft", J. of Aircraft Vol. 50 no. 4 , 1117-1130, 2013.

[8] Van den Hof, P "Closed-loop issues in system identification", Annu. Reviews in Control, Volume 22, Pages 173-186, 1998.

[9] Van der Hopf, P and Schrama, R.J.P, "Identification and Control- Closed loop issues" Automatica, Vol. 31, no 12, pp 1751-1770, 1995